Physica B 407 (2012) 2773–2777

Contents lists available at SciVerse ScienceDirect

Physica B

journal homepage: www.elsevier.com/locate/physb

Exchange bias in (1 1 0)-orientated $Bi_{0.9}La_{0.1}FeO_3/La_{0.5}Ca_{0.5}MnO_3$ films

J.L. Zhao, R.L. Gao, W.W. Gao, B.G. Shen, J.R. Sun *

Beijing National Laboratory for Condensed Matter Physics and the Institute of Physics, Chinese Academy of Sciences, Beijing 100190, PR China

ARTICLE INFO

Article history:
Received 28 February 2012
Received in revised form
10 April 2012
Accepted 13 April 2012
Available online 21 April 2012

Keywords:
Exchange bias
BLFO/LCMO films
Magnetic phases

ABSTRACT

We performed a systematic study on the exchange bias in (1 1 0)-orientated $Bi_{0.9}La_{0.1}FeO_3/La_{0.5}Ca_{0.5}MnO_3$ (BLFO/LCMO) heterostructure with a fixed BLFO film thickness of 600 nm and different LCMO layers ranging from $t=0$ to 30 nm. The LCMO is found to be weakly ferromagnetic, with the Curie temperature descending from ~225 K to 0 as the layer thickness decreases from 30 nm to 3 nm. The main magnetic contributions come from the BLFO film, and the areal magnetization ratio is 1:0.07 for $t=5$ nm and 1:0.82 for $t=30$ nm for BLFO to LCMO at the temperature of 5 K. Further experiments show the presence of significant exchange bias, and it is, at the temperature of 10 K, ~40 Oe for $t=0$ and ~260 Oe for $t=30$ nm. The exchange bias reduces dramatically upon warming and disappears above the blocking temperature of the spin-glasslike behavior observed in the samples. The possible origin for exchange bias is discussed.

1. Introduction

A multiferroic material is one which simultaneously possesses two or more ferroic order parameters [1]. $BiFeO_3$ (BFO) is a promising multiferroic oxide that has the ferroelectric and antiferromagnetic (AFM) transition temperatures well above room temperature [2]. For BFO, the ferroelectric polarization is strongly coupled to the spin structure, and electric field can affect the latter via changing the direction of the former [3]. This feature of the BFO has been incorporated into the ferromagnet/BFO heterostructure, tuning the exchange bias (H_{eb}) between BFO and ferromagnet [4].

In most of the previous works, BFO has been treated as an idealized AFM material [4,5], and the exchange bias is exerted on the ferromagnetic (FM) layer by BFO [4,6]. However, the magnetic property of BFO could be much more complex due to the presence of structural and compositional defects. As a consequence, magnetic inhomogeneity, canted/helical AFM spin structure, and parasitic FM state are possible. In fact, considerable net magnetization has been reported for the BFO compounds of different forms such as polycrystalline [7] and nanometer-sized materials [8]. Significant exchange bias was also observed in the $Bi_{1/3}Sr_{2/3}FeO_3$ polycrystalline [9] and $BiFe_{0.8}Mn_{0.2}O_3$ nanoparticles [10].

We noted that most of the previous studies concentrated on the exchange bias between the FM and BFO layers, and the works on $Bi_{1/3}Sr_{2/3}FeO_3$ and $BiFe_{0.8}Mn_{0.2}O_3$ are the only two reports for the exchange bias within the multiferroic oxides themselves. For this kind of exchange interaction, there are many issues to be addressed, such as the dependence of the H_{eb} on the form of the materials (bulk, nanometer-sized, and film materials) and the effect of electric field. As is well known, the measurement of the ferroelectric property is usually difficult for polycrystalline and nanometer-sized materials due to severe leakage. This limits a thorough exploration of the multiferroic character of the materials. Compared with bulk materials, BFO films are more attractive because of their particular importance for material engineering. Thin films are also suitable for the study of electric–magnetic coupling. However, the magnetic behavior, particularly the one associated with exchange bias, of thin films could be different from those of bulk materials due to lattice strains and interfacial defects, and a systematic study is required. In this paper we performed a comprehensive investigation on the exchange bias in (1 1 0)-orientated $Bi_{0.9}La_{0.1}FeO_3/La_{0.5}Ca_{0.5}MnO_3$ (BLFO/LCMO) film. The BLFO films of 600 nm in thickness were grown on the LCMO layer of different thicknesses (thus different magnetic properties) to check the effects of the underlayer. Here La has been incorporated into BFO to reduce leakage current. The LCMO film is chosen because of its distinctive magnetic property. At the FM–AFM phase boundary it is weakly FM [11]. The films are found to be weakly FM, with a maximal magnetization of ~3.8 emu/cm^3, mainly contributed by the BLFO film. Considerable exchange bias and its correspondence to the spin-glasslike (SGL) behavior are further observed. These results support the scenario of magnetic phase separation in BLFO, i.e. the coexistence of FM, SGL, and AFM phases in the films, with the former two phases probably located near grain boundaries.

2. Experiment

The samples have been fabricated by growing, via pulsed laser ablation, first a $La_{0.5}Ca_{0.5}MnO_3$ (LCMO) layer and then a $Bi_{0.9}La_{0.1}FeO_3$ (BLFO) film on (1 1 0)-orientated $SrTiO_3$ substrate. A BLFO target was

* Corresponding author. Tel.: +86 10 82648075.
E-mail address: jrsun@aphy.iphy.ac.cn (J.R. Sun).

0921-4526/$ - see front matter © 2012 Elsevier B.V. All rights reserved.
http://dx.doi.org/10.1016/j.physb.2012.04.025

prepared with ~15% excessive Bi to compensate for the high volatilization of Bi. During the deposition, the temperature was kept at 650 °C (720 °C) and the oxygen pressure at ~15 Pa (~46 Pa) for the BLFO (LCMO) film. The thickness is 600 nm for the BLFO film and varies from $t=0$ to 30 nm for the LCMO layer, controlled by deposition time. After the deposition, the films are cooled to room temperature very slowly (~5 °C/min) in an oxygen atmosphere of ~500 Pa.

The structure of the films was analyzed by a X-ray diffractometer with the Cu Kα radiation (Brüker AXS D8 Discovery X-ray diffractometer). The surface morphology was measured by atomic force microscopy (AFM, Nanonavi E-Sweep). The *P–E* hysteresis of the films was measured using a Radiant Premier II tester (Radiant Technologies, Inc., Albuquerque, NM). Magnetic measurements were carried out on a MPMS SQUID VSM dc Magnetometer (Quantum Design).

3. Results and discussion

Fig. 1(a) shows the semi-log plot θ–2θ X-ray diffraction spectrum of the film LCMO (30 nm)/STO(1 1 0) recorded at room temperature. In addition to those of the substrate, only the diffraction peaks of LCMO can be detected for the 2ϑ angle from 25° to 75°, and no fine structure of the (n n 0) LCMO peaks was resolved. The inset shows an AFM image (height data) of the free surface with a scanning area of 4×4 μm^2, indicating a continuous and smooth film surface, with the root-mean-square roughness 0.76 nm. Fig. 1(b) shows the X-ray diffraction spectrum of sample $t=5$ nm. It confirms the single-phase character of the BLFO films and the same crystallographic orientation of the film as the substrate. The deduced lattice constant is $d_{110}/\sqrt{2}=3.990$ Å (assuming $a=b$), essentially independent of the LCMO layer thickness. The left and right insets in Fig. 1(b) are magnified (1 1 0) peaks for two typical samples and the corresponding rocking curves. The full width at half height of the (1 1 0) peak is nearly identical for both films, ~0.21°, whereas the rocking curves are slightly different, ~0.13° for $t=5$ nm and ~0.17° for $t=30$ nm (the peak width of the rocking curve of the $SrTiO_3$ substrate is ~0.1°). It seems that the variation of the LCMO layer thickness affects the quality of the films.

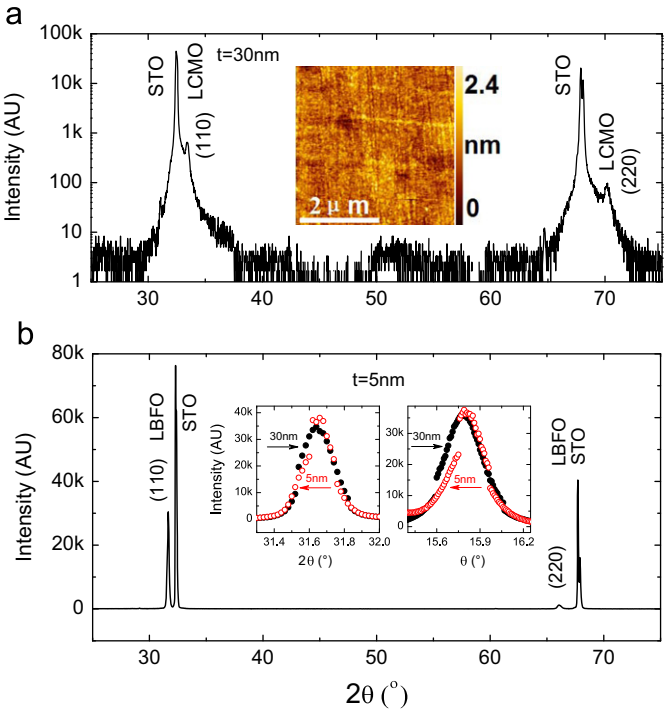

Fig. 1. (a) θ–2θ X-ray diffraction spectrum of the film LCMO(30 nm)/ STO(1 1 0) recorded at room temperature. No fine structure of the (n n 0) LCMO peaks was resolved. The inset shows an AFM image (height data) of the free surface. (b) θ–2θ X-ray diffraction spectrum of the film BLFO/LCMO(5 nm) recorded at room temperature. In addition to those of the substrate, the diffraction peaks of the BLFO film can be clearly seen (the LCMO layer is too thin to be detected). The left inset is a close view of the (1 1 0) peaks for two typical samples of $t=5$ nm and 30 nm. The right inset shows the corresponding rocking curves. STO denotes the $SrTiO_3$ substrate.

Fig. 2(a) shows the ferroelectric polarization–electric field (*P–E*) curves of the typical film BLFO/LCMO(30 nm), measured at room temperature. Although the *P–E* curve is not shaped as squarely as expected, the polarizing process can still be clearly seen. The maximal polarization is ~7 μC/cm^2 under the field of 100 MV/m, lower than the optimal value of the LBFO films (~80–100 μC/cm^2). The coercive force is ~45 MV/m, greater than that reported for the BFO film (~20 MV/m) [2]. The actual electric field in BLFO may be lower than 100 MV/m, which is obtained simply by dividing the voltage applied to the sample by the film thickness of BLFO, without considering voltage drop on LCMO, which could be significant since LCMO is highly resistive (the resistance is 30 kΩ while the dimension of the LCMO layer is 3×2 mm^2).

To get the information on the magnetic properties of the BLFO film, the temperature-dependent magnetization *M–T* was measured under the field of 0.1 T in field-cooled (FC) mode (Fig. 2(b)). Here the areal magnetization is adopted to show the relative contributions of the BLFO and LCMO films. *M* displays a smooth growth with the decrease of temperature when the layer thickness of LCMO is below 3 nm. This result suggests the absence of the contributions from the LCMO layer (the magnetization of the $SrTiO_3$ substrate is in the order of 3×10^{-5} emu/cm^2, and can be neglected). However, a visible magnetic anomaly appears in the *M–T* relation of the sample $t=5$ nm, leading to an enhanced inclining of the *M–T* curve below ~165 K (marked by shaded area). This feature develops as *t* increases, and results in a sudden

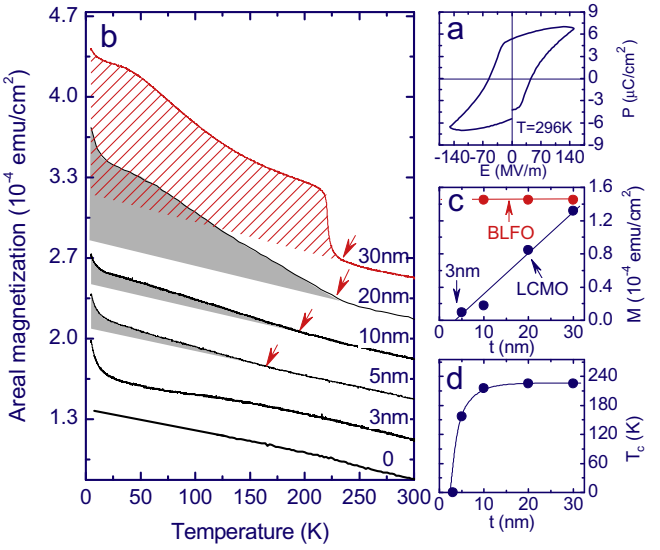

Fig. 2. (a) Ferroelectric polarization of the BLFO/LCMO(30 nm) film as a function of electric field, measured at the room temperature. (b) Temperature-dependent magnetization of the BLFO/LCMO films, measured under the field of 0.1 T in the field-cooled mode. Upward shifts of the *M–T* curves for $t>0$ have been taken for clarity. Shaded areas mark the contributions of LCMO. The Curie temperature of LCMO is denoted by arrows. (c) Magnetization as a function of layer thickness of LCMO and BLFO, collected at 5 K. (d) Curie temperature of LCMO as a function of layer thickness. Solid lines are guides for the eye.

magnetization jump at ~230 K when $t=30$ nm. These results signify the emergence and development of the FM order of the LCMO layer. The magnetization of LCMO can be obtained by subtracting the data of BLFO from those of BLFO/LCMO. As shown in Fig. 2(c), it is $\sim 1.3\times10^{-4}$ emu/cm^2 for $t=30$ nm, linearly decreased to $\sim 1.0\times10^{-5}$ emu/cm^2 for $t=5$ nm, and undetectable below the thickness of 5 nm. Correspondingly, the Curie temperature of the LCMO layer, marked by the inflection point in the M–T curve, varies regularly, ascending from ~165 K to ~230 K as t grows from 5 to 30 nm (Fig. 2(d)). In contrast, the magnetization of the BLFO film is considerably large ($\sim 8.3\times10^{-5}$ emu/cm^2 at 300 K and $\sim 1.47\times10^{-4}$ emu/cm^2 at 5 K), and is essentially independent of the thickness of the LCMO layer. A simple calculation shows the magnetization ratio M_{BLFO}:M_{LCMO}=1:0.82 for $t=30$ nm and 1:0.07 for $t=5$ nm when $T=5$ K. Therefore, the magnetic contribution comes mainly from the BLFO film when t is small.

To get the knowledge on the magnetic structure of the BLFO films, we studied the irreversible behavior by measuring magnetization in different cooling modes. Fig. 3(a) and (b) illustrates the magnetizations as a function of temperature for typical samples $t=3$ nm and 30 nm, recorded in a field of 0.05 T in the zero-field-cooled (ZFC) and FC modes, respectively. The FC magnetization shows a monotonic growth upon cooling whereas the ZFC one exhibits a broad maximum at ~125 K or ~50 K (varying with t). These results indicate, in addition to the imperfection of the FM order, the occurrence of spin freezing in the low temperature region, a typical feature of spin glass. The bifurcation of the ZFC and FC curves appears well above the blocking temperature, which implies a high ordering temperature for the BLFO film.

BFO has been treated as an idealized AFM material in most of the previous works. However, the experiment results here reveal the complexity of the magnetic behavior of BLFO. As is well known, in addition to the idealized spin–glass system, the SGL behavior usually appears in phase-separated materials. It is worthwhile to check whether there are any effects with the feature of phase separation in the BLFO film. For this purpose, in the following we will focus on the possible exchange bias experienced by the BLFO or LCMO films. To reveal the effects of exchange bias, we measured the magnetization of the BLFO film while cycling the field along the route $0\rightarrow0.3\ \mathrm{T}\rightarrow0\rightarrow-0.3\ \mathrm{T}\rightarrow0$ after cooling the sample from 350 K to 10 K in the fields $H=0$ or ±1 T. Fig. 4(a) and (b) shows the M–H curves of two typical samples $t=3$ nm and 30 nm, respectively. Positive (negative) field cooling causes a left (right) shift of the M–H curves and an obvious increment in saturation magnetization (ΔM_S). These results suggest the presence of exchange bias, which pushes forwards or backwards the spin flip of the FM phase. Fig. 4(c) exemplifies the exchange bias, defined as half of the difference of the positive and

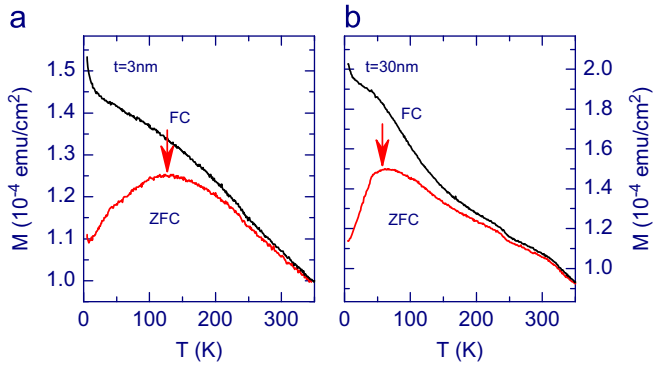

Fig. 3. Areal magnetization as a function of temperature for the BLFO/LCMO(t) films of $t=3$ nm (a) and 30 nm (b), measured under an applied field of 0.05 T in the ZFC and FC modes. Arrows mark the blocking temperature.

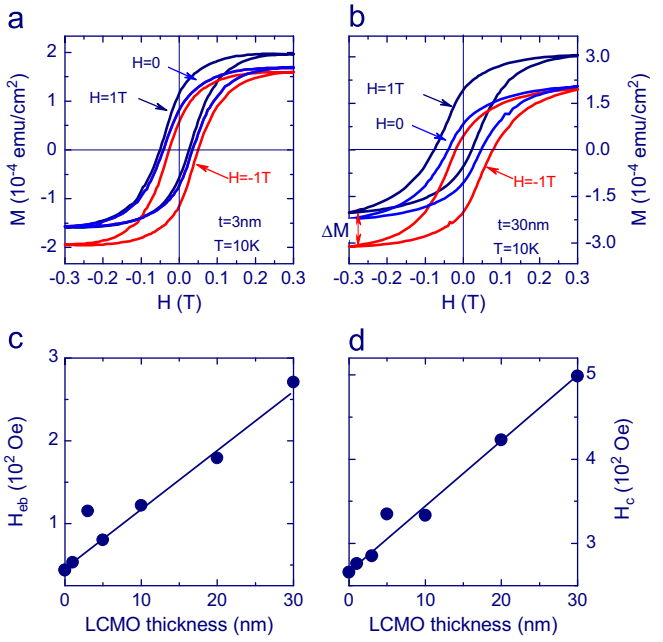

Fig. 4. Magnetization–magnetic field relation for the BLFO/LCMO(t) films with the layer thickness of LCMO of $t=3$ nm (a) and 30 nm (b). Filed-induced anisotropic elongation of the M–H curves is observed. Exchange bias and coercive fore are respectively presented in (c) and (d), as functions of the layer thickness of LCMO. Solid lines are guides for the eye.

negative forces (H_c), as a function of the layer thickness of LCMO. H_{eb} is fairly large, and it is ~45 Oe for $t=0$ and ~270 Oe for $t=30$ nm at the temperature of 10 K. Correspondingly, the coercive force varies from ~270 Oe to ~500 Oe (Fig. 4(d)).

In general, an exchange bias exists at the interface of the FM and AFM phases. As reported by Wu et al. [4], the exchange bias at the $La_{0.7}Sr_{0.3}MnO_3$–$BiFeO_3$ interface is ~225 Oe at the temperature of 7 K (the thickness of the $La_{0.7}Sr_{0.3}MnO_3$ film is 5 nm), and undergoes a monotonic decrease with the film thickness of LSMO. It may not be the case here because of the following reasons: first, the magnetization detected is contributed mainly by the BLFO film rather than the LCMO film, especially when the latter is thin. This implies that the M–H curves describe the magnetic behaviors of BLFO rather than LCMO. Second, the behavior of the exchange bias deviates obviously from the relation predicted by $H_{eb}\propto1/t$ that describes the exchange bias at the FM–AFM interface [12]. The monotonic growth of H_{eb} with t observed here means that the exchange bias is not limited to the BLFO–LCMO interface. The exchange bias observed here may occur within the BLFO film, originating from the magnetic coupling between different phases in BLFO, i.e., the results obtained suggest a scenario of phase separation. In fact, because of the inhomogeneous distribution of structural and compositional defects, different phases can be formed in BFO and related oxides. As reported, the AFM $BiFe_{0.8}Mn_{0.2}O_3$ nanoparticles [10] and Co_3O_4 nanowires [13] exhibit a core–shell magnetic structure, i.e., AFM cores plus surrounding diluted AFM layers (DAF). The DAF phase can be further driven into the SGL or even weakly FM phase by severe structure/composition defects.

According to the atomic force microscopy analysis, the average grain size is ~0.2 μm for the BLFO films, smaller than that in polycrystallites (several micrometers). For the BLFO films, defects may concentrate on the regions near grain boundaries and, on the analogy of nanometer-sized materials, they may lead to magnetic inhomogeneity and parasitic FM state. It is possible that the FM phase is formed in regions with high defect content, probably the outmost layer of the grains. There may be a transition layer,

i.e., SGL or DAF phase, intermediate between the FM and AFM phases, and it is the coupling between the FM and SGL (DAF) phase that produces the exchange bias.

As is well established, exchange coupling can exist between frozen out and free spins [14], which slugs the response of the latter to external field. Indeed, the exchange bias observed here shows a close relation to spin freezing. As shown by Figs. 3 and 5, it emerges when spins are frozen out, reduces rapidly upon warming, and nearly completely disappears when the pinned spins are thermally freed. These features are particularly clear in sample $t=30$ nm. For the sample 3 nm, although exchange bias remains visible at high temperatures, the most rapid change occurs below the freezing point ($\sim$130 K).

The increase of the saturation magnetization may be understood in the scenario that part of the uncompensated spins in the SGL layer couples with those of the FM phase, rotating during the magnetization reversal. According to Fig. 6, the saturation magnetization growth induced by cooling field is quite large, $\sim$8.3% for $t=3$ nm and $\sim$25% for $t=30$ nm. The FM phase may prefer to form around the grain boundaries, separated from the AFM core by the SGL interfacial layer. In this case, the FM phase has the maximal FM–SGL interface, and the number of the affected spins in the SGL phase in the field cooling process is large.

There are two explanations for the phenomena associated with the exchange bias. One is based on the existence of two kinds of spins in the SGL phase. The first kind of spins weakly couples to the spins of the FM phase, contributing to saturation magnetization, and the second kind spins pin the FM phase, yielding the exchange bias. The second explanation is based on the assumption of the coupling, which gives rise to the exchange bias, between rotatable and frozen spins in the SGL phases without assuming the interaction between the frozen spins in the SGL phase with that of the FM phase. In the later case, the field-induced magnetization increment ΔM_S should have a close relation to exchange bias. A large ΔM_S means a large number of spins that are aligned by magnetic field. If all these spins participate in the pinning of the FM phase, H_{eb} will be proportional to ΔM_S. This phenomenon is indeed experimentally observed. As illustrated by Fig. 4, H_{eb} shows a linear increase with ΔM_S at a speed of $\sim 1.2\times10^{-6}$ Oe cm^2/emu, and there will be no exchange bias for $\Delta M_S=0$.

We also measured the thermoremanent magnetization (TRM) and isothermoremanent magnetization (IRM) at 5 K in the field range from 0 to 7 T. To measure the TRM the sample is FC from room temperature down to 5 K, the field is removed, and then the magnetization recorded. To measure the IRM the sample was ZFC from room temperature down to 5 K, the field was then swiftly applied, removed again, and the remanent magnetization recorded. Fig. 7 shows the results for the typical sample $t=3$ nm. According to this figure, both the TRM and IRM experience first a rapid and then a smooth growth with increasing applied field. However, the TRM is always greater than the IRM. This is a typical feature of the system with exchange bias, and the TRM and IRM difference is contributed by the robust spins that yield the H_{eb}. It is interesting to note the visible hump in the Δ–T relation (Δ=TRM–IRM) in the inset plot in Fig. 7. It may be an indication for the SGL, rather than DAF, character of the interfacial phase. As is well established, for the typical spin-glass system, the difference of the TRM and IRM exhibits a significant peak in low fields [15].

An alternative picture for the exchange bias is that the AFM grain is uniformly canted while the outmost layer of the grain is in the SGL state, and the magnetization comes from the AFM core and the exchange bias from the SGL–AFM interaction. However, in this case the exchange bias could be quite low, and cannot explain the experiment results. As is well known, the effect of exchange bias exists at the interface of different phases, and usually extends only several nanometers. The SGL layer could not pin the AFM core as thick as 0.1–0.2 μm (the size of the grain).

The universal dependence of H_{eb} on t is worth nothing. As experimentally revealed, the M–H curve reflects mainly the behavior of the BLFO film when $t\leq10$ nm whereas a combined behavior of the BLFO and LCMO films when $t\geq20$ nm. The absence of visible anomalies when t sweeps through 20 nm implies that BLFO and LCMO form a unified system with the core–shell-like exchange bias. It seems that exchange coupling in BLFO has extended to the whole LCMO film via interlayer coupling.

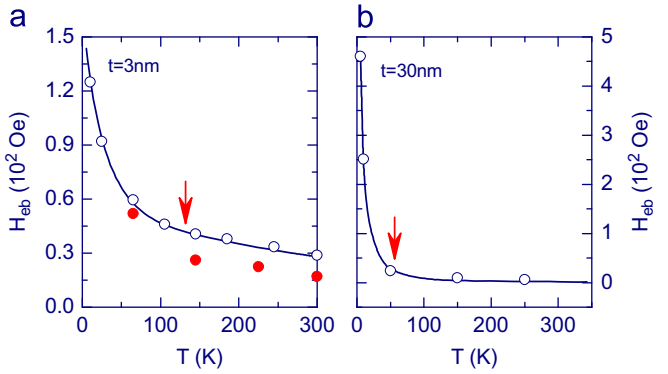

Fig. 5. Exchange bias of the BLFO/LCMO(t) films with the layer thickness of LCMO of $t=3$ nm (a) and 30 nm (b), as a function of temperature. Solid lines are guides for the eye.

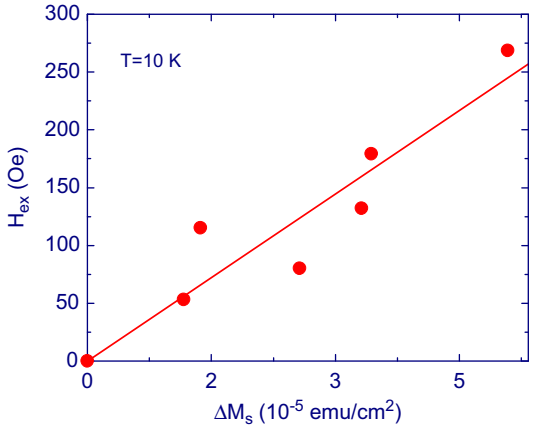

Fig. 6. Relation between exchange bias and field-induced increment in saturation magnetization, recorded at a fixed temperature of 10 K.

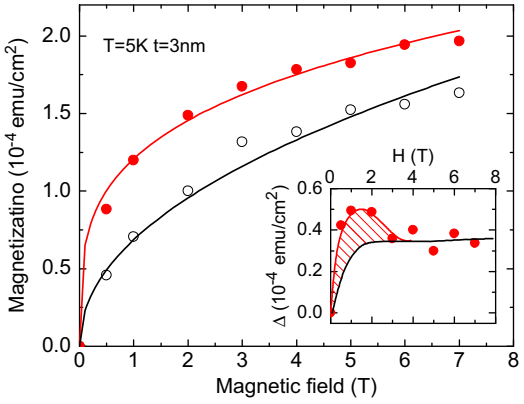

Fig. 7. TRM and IRM as functions of magnetic field, measured at a fixed temperature of 5 K. Inset plot shows the difference of the TRM and IRM. Shaded area marks the anomaly due to the SGL phase. Solid lines are guides for the eye.

The increase of exchange bias with the layer thickness of LCMO may be a consequence of the change of the crystal quality of the BLFO film. Since the widths of the θ–2θ peaks are mainly determined by film thickness of BLFO, no obvious changes are observed as t varies. However, the rocking curves broaden slightly as t grows. This actually suggests a disordering of the crystallographic orientation of the film, which may directly affect the microstructure of grain boundaries.

As well known, the coercive force of the magnetic material with structure defects is mainly determined by domain wall pinning, and it is the magnetic field required to amend the orientation of the domain wall spins. This may be the case occurring in the BLFO/LCMO films. The growth of H_c with t implies a strengthening of spin pinning, and thus an enhanced disordering of the microstructure at grain boundaries in the sample with thick LCMO layers. As for the reason for the increase in misaligned spins as t grows, it may be a consequence of enhanced grain boundary disordering. As revealed by the atomic force microscope analysis, the root-mean-square roughness of LCMO increases with film thickness, growing from $\sim$0.56 nm to $\sim$0.76 nm as t increases from 0 to 30 nm, which may lead to an enhanced disordering in the microstructure of the above BLFO film.

4. Conclusion

In summary, we performed a systematic study on the exchange bias in (1 1 0)-orientated $Bi_{0.9}La_{0.1}FeO_3/La_{0.5}Ca_{0.5}MnO_3$ (BLFO/LCMO) heterostructure with a fixed BLFO film thickness of 600 nm and different LCMO layers ranging from 0 to 30 nm. The LCMO is found to be weakly ferromagnetic, with the Curie temperature descending from $\sim$225 K to 0 as the layer thickness decreases from 30 nm to 3 nm. The main magnetic contributions come from the BLFO film when the LCMO layer is thin, and the maximal ratio of the areal magnetization of BLFO to LCMO is about 1:0.82 and 1:0.07 for the LCMO layer of 30 nm and 5 nm, respectively. Significant exchange bias is detected. It is $\sim$40 Oe at the temperature of 10 K without LCMO and grows to $\sim$260 Oe as the LCMO layer thickness increases from 0 to 30 nm. It reduces dramatically upon warming and disappears above the freezing temperature of the spin-glasslike behavior observed in the samples. The exchange bias may mainly exist between different magnetic phases in the BLFO film. These results support the inhomogeneous magnetic scenario in the BLFO films, i.e. the coexistence of FM, SGL, and AFM phases in the films, with the two former phases probably being formed around grain boundaries. The possible origin for exchange bias is discussed.

Acknowledgment

JRS would like to thank Professor J.W. Cai for valuable discussions. This work has been supported by the National Basic Research of China, the National Natural Science Foundation of China, the Knowledge Innovation Project of the Chinese Academy of Science, and the Beijing Municipal Nature Science Foundation.

References

[1] Y. Tokura, Science 312 (2006) 1481;
R. Ramesh, Nicola A. Spaldin, Nat. Mater. 6 (2007) 21.
[2] J. Wang, J.B. Neaton, H. Zheng, V. Nagarajan, S.B. Ogale, B. Liu, D. Viehland, V. Vaithyanathan, D.G. Schlom, U.V. Waghmare, N.A. Spaldin, K.M. Rabe, M. Wuttig, R. Ramesh, Science 299 (2003) 1719.
[3] Ying-Hao Chu, L.W. Martin, M.B. Holcomb, M. Gajek, Shu-Jen Han, Qing He, N. Balke, Chan-Ho Yang, Donkoun Lee, Wei Hu, Qian Zhan, Pei-Ling Yang, A. Fraile-Rodríguez, A. Scholl, S.X. Wang, R. Ramesh, Nat. Mater. 7 (2008) 478; T. Zhao, A. Scholl, F. Zavaliche, K. Lee, M. Barry, A. Doran, M.P. Cruz, Y.H. Chu, C. Ederer, N.A. Spaldin, R.R. Das, D.M. Kim, S.H. Baek, C.B. Eom, R. Ramesh, Nat. Mater. 5 (2006) 823.
[4] S.M. Wu, S.A. Cybart, P. Yu, M.D. Rossell, J.X. Zhang, R. Ramesh, R.C. Dynes, Nat. Mater. 9 (2010) 756.
[5] G.A. Smolenskii, I.E. Chupis, Sov. Phys. Usp. 25 (1982) 475.
[6] J. Allibe, I.C. Infante, S. Fusil, K. Bouzehouane, E. Jacquet, C. Deranlot, M. Bibes, A. Barthélémy, Appl. Phys. Lett. 95 (2009) 182503.
[7] Q.Y. Xu, H.F. Zai, D. Wu, T. Qiu, M.X. Xu, Appl. Phys. Lett. 95 (2009) 112510.
[8] S. Basu, S.K.M. Hossain, D. Chakravorty, M. Pal, Curr. Appl. Phys. 11 (2011) 976.
[9] Z.M. Tian, S.L. Yuan, X.F. Zheng, L.C. Jia, S.X. Huo, H.N. Duan, L. Liu, Appl. Phys. Lett. 96 (2010) 142516.
[10] P.K. Manna, S.M. Yusuf, R. Shukla, A.K. Tyagi, Phys. Rev. B 83 (2011) 184412.
[11] A.J. Millis, Nature 392 (1998) 147;
P. Levy, F. Parisi, G. Polla, D. Vega, G. Leyva, H. Lanza, Phys. Rev. B 62 (2000) 6437;
M. Malfait, I. Gordon, V.V. Moshchalkov, Y. Bruynseraede, G. Borghs, P. Wagner, Phys. Rev. B 68 (2003) 132410.
[12] J. Nogués, Ivan K. Schuller, J. Magn. Magn. Mater. 192 (1999) 203.
[13] M.J. Benitez, O. Petracic, E.L. Salabas, F. Radu, H. Tüysüz, F. Schüth, H. Zabel, Phys. Rev. Lett. 101 (2008) 097206.
[14] Young Yan-kun Tang, Sun, Zhao-hua Cheng, Phys. Rev. B 73 (2006) 174419.
[15] J.L. Tholence, R. Tournier, J. Phys. (Paris) Colloq 35 (1974) C4.